Franciszek WITOS[1], Agnieszka LISOWSKA-LIS[2]

# 21. THE IDENTIFICATION OF SIGNALS AND LOCATION OF SOURCES OF PARTIAL DISCHARGES AND MAGNETIZATION PROCESSES IN OIL POWER TRANSFORMERS BY MEANS OF ACOUSTIC EMISSION METHOD

## 21.1. Introduction

Oil power transformers are important elements of the power system and detailed rules for their operation have been developed [1]. The Framework Instruction for Operation of Transformers divides transformers into four groups, whereby oil power transformers are included in group I (oil transformers with an primary rated voltage of 220 kV and higher or power of 100 MVA and higher), group II (oil transformers with a power greater than 1.6 MVA, not included in group I) and group III (power oil transformers up to 1.6 MVA). The Framework Instruction for Operation of Transformers specifies technical tests of transformers by specifying types of tests, test methods and evaluation criteria. The program of operational tests includes three stages, i.e. basic, specialist and periodic tests. In the area of specialist and periodic tests for transformers of groups I and II, tests performed without disconnecting the transformer from the network play an important role. These include chromatographic analysis of dissolved gases (DGA), partial discharge (PD) measurement by acoustic emission (AE) method, vibroacoustic analysis, thermovision tests and tests of the content of furan compounds dissolved in oil.

The transformer failure statistics show that the main causes of failures are [2, 3]:

a) insulation system failures (42%),
b) damage of bushings and their flexible connections with the phase lead of the winding (23%),
c) damage to the on-load tap-changer (17%),

[1] Department of Optoelectronics, Faculty of Electrical Engineering, Silesian University of Technology, Krzywoustego 2, 44-100 Gliwice, Poland, franciszek.witos@polsl.pl
[2] Department of Electrical Engineering, Polytechnic Faculty, University of Applied Sciences in Tarnow, Mickiewicza 8, 33-100 Tarnów, Poland, lisowskalis@pwsztar.edu.pl

d) other, e.g., reduction of oil operating parameters as a result of moisture, "overheating" in electrical connections of windings, short-circuiting of metal sheets in a magnetic circuit (18%)

The above statistics indicate that the majority of power network failures are caused by electrical insulation failure, and the key indicator of such failure is the occurrence of PD. Therefore, one of the goals of condition monitoring is to detect PD, especially in the early stages, to prevent a major power failure or failure. The AE method has such possibilities and is used in on-line tests of oil-filled power transformers [4-8]

The paper presents the results of tests of a selected oil transformer indicating the identification of PD signals and the location of the PD sources (analysis of recorded signals in the 100-200 kHz band) as well as identification of signals from the magnetization processes taking place in the magnetic circuit of the transformer and the location of their sources (analysis of recorded signals in the band 20-100 kHz).

## 21.2. Research method, measurement system and tested object

In a working oil power transformer there are numerous phenomena, the occurrence of which causes acoustic impulses to be generated in the sources and then propagated in the volume of the transformer as acoustic signals. They are:

a) acoustic emission (AE) signals generated during deformation processes that accompany partial discharges (PDs) [4, 5, 8, 11-13],
b) magnetoacoustic emission (MAE) signals generated by numerous phenomena that occur during the magnetization of the ferromagnetic materials] [14-16],
c) acoustic signals generated during oil circulation in the transformer,
d) vibroacoustic signals,
e) outer acoustic interference.

The study of acoustic signals that are generated by the modeled sources led to the following conclusions:

- in the 100-200 kHz band, signals from acoustic phenomena that accompany partial discharges are dominant,
- in the 20-100 kHz band, there are acoustic signals from many phenomena, such as, among others, acoustic phenomena that accompany partial discharges, phenomena associated with the process of the magnetization of ferromagnetic materials and acoustic phenomena generated by the circulation of the transformer’s oil,
- the 20-40 kHz band is the dominant band for acoustic signals generated during some types of partial discharges and during phenomena associated with the magnetization process of ferromagnetic materials.

The acoustic emission test method that was used (author's patented research method - Patent PL223 606, Oct. 2016) consists of the following elements:

- an 8AE-PD measurement system,
- the construction of a network of measurement points on the side walls of the transformer's oil tank,
- mounting the AE sensors,
- checking the quality of the mounting of individual sensors using the Hsu-Nielsen method,
- analysis of the properties of the acoustic emission signals generated during the Hsu-Nielsen tests,
- data recording,
- determining the author's maps of the descriptors on the side walls of the tested transformer, together with the location of the areas with increased acoustic emission activity,
- analysis of the properties of the acoustic emission signals recorded at the measurement points in areas identified as local maxima on the descriptor maps along with identification of the sources of the registered signals.

During the investigation, the 8AE-PD measurement-research system was used [9, 10]. It is a computer measurement system dedicated to locating and describing PDs in oil power transformers using the acoustic emission method. This system has 8 independent measurement channels; simultaneous recording of the signals in up to all 8 measurement channels is possible and it provides the opportunity to locate the source of AE signals. The gain of the system is fully controlled by its software, with a dynamic range of 65 dB for input signal changes (preamplifier + amplifier). The bandwidth of the system is from 20 kHz to 1000 kHz. The system is equipped with the authors' software which was written in LabVIEW which enables:

- monitoring of the signals,
- recording of the data in real time (within the band of 20-1000 kHz),
- basic (in the domains of time, frequency and time-frequency) and advanced (in the domains of discrimination threshold) analysis of the recorded signals.

The limit values of the apparent charge introduced by the PD source, for which the recorded signal can be identified as that coming from the PDs, is 20 pC for the 8AE-PD computer measurement system [9, 10].

The block diagram of the measurement 8AE-PD system with the eight CH0-CH7 measurement channels, together with the AE sensors (TR0-TR7 respectively) in these channels is shown in Fig. 1.

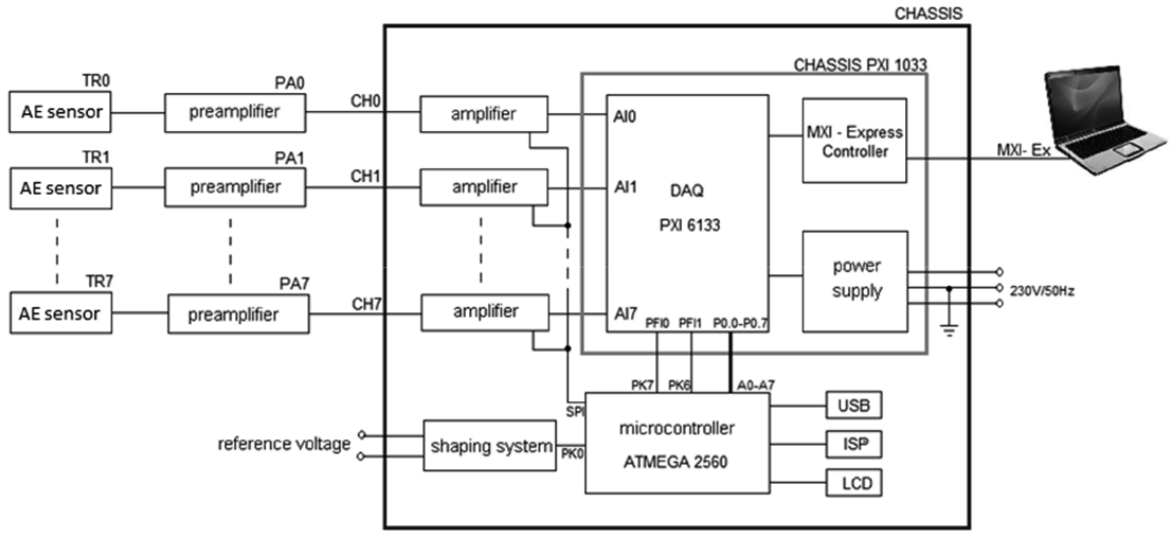


Fig. 1. Block diagram of the measurement 8AE-PD system
Rys. 1. Schemat blokowy układu pomiarowego 8AE-PD

Fig. 2. Diagnosed oil power transformer
Rys. 2. Widok diagnozowanego olejowego transformatora energetycznego

The diagnosed object (Fig. 2) was an oil cooled power transformer; the transformer has been operating for over 40 years. Its parameters are: 110/15/6 kV winding voltages (YNd11d11), 50 Hz, 40 MVA; Nominal power: 40000/25000/25000 kVA; Oil mass of 21800 kg and total mass of 72000 kg. The power load of the transformer is about 40-50% of its nominal power and this is a typical power load for regular work of the power transformers in the distribution system. During the measurements the current was 35 A (110 kV voltage)

and 280 A (15 kV voltage); 6 kV winding was not loaded. The transformer is oil cooled and oil circulation in the tank is powered by a circulating pump.

## 21.3. Carrying out measurements

In acoustic measurements, the installation of the sensor has a fundamental and direct impact on the values of the measured quantities because the values of the recorded quantities are affected by the coupling layer (its size, shape and quality). In addition to the AE method, when the sensors are mounted on the side walls of the power transformer's oil tanks, the pressure of the sensor to ensure a stable mounting of the sensor is important (while the sensor slides down, additional signals are generated, disturbing the measured values). The author of this work is a co-author of the PL Patent, number 223 606, Oct. 2016.

The author of this paper has been licensed as AT level 2 since 2015 and performed tests of over 30 pressure devices using the Vallen 32 multi-channel measurement system AMSY-6. In several studies, measurements were carried out with the 8AE-PD system simultaneously, gaining additional experience in conducting research [17]. Using the 8AE-PD measurement system, several oil power transformers were tested using the AE method [5-6, 18-20].

The obtained experience led to the final formulation of the course of the research of oil power transformers by the AE method. First, a network of measurement points is planned on the side walls of the transformer tank. It is created as follows:

a) during the first installation of the set of eight sensors (working in the eight measurement lines of the 8AE-PD system), seven AE sensors of the D9241A type are placed in the lower part of the vat, in one horizontal line (line 1) at intervals of about one meter, and the eighth sensor, i.e. the broadband AE sensor of the WDI type is placed near the sensor, which indicates the highest value of the recorded AE signal,
b) in subsequent mountings of the set of eight sensors, sensors are shifted in parallel by about 0.5 meters vertically along the side wall of the tank (lines 2,3, 4 ... until reaching the measurement points in the upper part of the tank which are available for measurements),
c) after completing the tests at the measuring points specified in point b, return to the level of line 1, move the set of sensors to new positions so that the measuring points cover the adjacent area of the tank and carry out appropriate measurements as described in points a and b,
d) the measurements described in point c are carried out so that the measurement points cover the side walls of the tank of tested transformer.

For each arrangement of a set of eight sensors, measurements are carried out to check the quality of the mounting of individual sensor using the Hsu-Nielsen method in accordance with the requirements of the PN-EN 14584:2013-07 Standard. The good quality of the installation of the set of sensors requires that for each sensor the measured peak-to-peak

amplitudes $U_{pp}$ value is within the range (mean $U_{pp}$ value calculated for the set of sensors – 3 dB, mean $U_{pp}$ value calculated for the set of sensors + 3 dB). If the requirements of the PN-EN 14584:2013-07 Standard are not fulfilled by the set of sensors, some of sensors are re-mounted at the same measuring points.

After obtaining a positive result when checking the quality of the mounting of the AE sensors (for each particular configuration), the AE signals reaching the AE sensors are recorded. Then ten signals are recorded at each measurement point; each signal has a duration of one second (approximately 50 cycles of the voltage supplying the transformer).

## 21.4. Results of analyzes of recorded data

### 21.4.1. Properties of the AE signals generated during the Hsu-Nielsen tests

Hsu-Nielsen test consists of breaking a 0.5 mm (alternatively 0.3mm) diameter pencil lead having length 3 mm (+/- 0.5 mm) from its tip by pressing it against the surface of the piece. This generates an intense acoustic signal which the sensors detect as a strong burst. These signals are characterized by high repeatability and reproducibility [21] and they are established standards as a reproducible AE sources [22].

At the moment of lead breakage, the accumulated stress is suddenly released, which causes a microscopic displacement of the surface and causes an acoustic wave that propagates into the structure. This wave contains mods from the complete system of solutions to the corresponding problem of elastodynamics. For the plate these mods are longitudinal wave, shear wave, and Lamb mods.

In Table 1 the AE sensors location (for one of particular configuration) and parameters of AE signals are given (peak-to-peak amplitudes $U_{pp}$ and ADC descriptor values) recorded with sensors mounted at a distance of 5 cm from Hsu-Nielsen sources, calculated after filtering the recorded signals in two frequency bands: 20-100 kHz and 100-200 Hz. 4th order bandpass filters were used for filtration. In separate rows, peak-to-peak amplitudes $U_{pp}$ of AE signals calculated within $dB_{AE}$ and the average values calculated for set of seven D9241A, are given.

For both frequency bands, the peak-to-peak amplitudes of $U_{pp}$ of AE signals are in the range (the average values for the set - 3 dB, the average values for the set + 3 dB). Such results confirmed the good quality of the installation of the AE sensors - in accordance with the requirements of the PN-EN 14584: 2013-07 Standard.

The properties of the signals recorded by the AE sensors for the active Hsu-Nielsen source next to the TR3 sensor are shown in Fig. 3 and in Table 2. The longitudinal wave has the highest velocity, therefore it is recorded first by the sensor. In Fig. 3, the times of arrival of the longitudinal wave to individual sensors are marked as $t_{20}$, $t_{30,}$ $t_{50}$, respectively, and the calculated longitudinal wave propagation speeds in the transformer tank for both frequency

bands are identical and have the value $v_L$ = 5700 m/s. Out of value recorded amplitudes, it is visible that most of the energy of the generated modes is propagated in Lamb modes.

Table 2 shows changes in peak-to-peak amplitudes $U_{pp}$ with a change in the length of the propagation path. These amplitude changes are due to the change in wave amplitude during propagation, wave attenuation during propagation and the radiation of some of the wave energy into the oil in the tank. These cumulative wave amplitude changes can be described by AE attenuation coefficients for the individual frequency. The calculated AE attenuation coefficients are as follows: $\beta$ (20-100 kHz) = 0.92 dB/m, $\beta$ (100-200 kHz) = 2.78 dB/m and show that the coefficient in the upper frequency band is three times greater than in the lower frequency band.

For comparison, in the measurements carried out for the modeled PD sources placed in oil inside the tank at a distance of about 50 cm from the tank on which sensors type D9241A were mounted, the recorded signals after filtration in the 100-200 kHz band had the following ADC descriptor values: ADC (400 pC) = -530, ADC (200 pC) = -1400 [10].

Table 1

The AE sensors location (for one of configuration) and parameters of AE signals (peak-to-peak amplitudes $U_{pp}$ and ADC descriptor values) recorded with sensors mounted at a distance of 5 cm from Hsu-Nielsen sources

| AE sensor | type of AE sensor | location *X* | location *Y* | measuring channel | CHn(H-Nn) 20-100 kHz | | | CHn(H-Nn) 100-200 kHz | | |
|---|---|---|---|---|---|---|---|---|---|---|
| | | cm | cm | | *Upp* mV | *Upp Db* | *ADC* a. u. | *Upp* mV | *Upp* dB | *ADC* a. u. |
| TR0 | D9241A | -615 | 90 | CH0 | 229.4 | 47.3 | -22.1 | 111.3 | 41.1 | -38.5 |
| TR1 | D9241A | -545 | 90 | CH1 | 204.9 | 46.4 | -25.9 | 115.5 | 41.2 | -38.5 |
| TR2 | D9241A | -481 | 90 | CH2 | 204.0 | 46.4 | -27.9 | 114.1 | 41.1 | -41.2 |
| TR3 | D9241A | -350 | 90 | CH3 | 230.4 | 47.3 | -24.0 | 120.2 | 41.4 | -37.0 |
| TR4 | D9241A | -290 | 90 | CH4 | 196.9 | 46.3 | -26.8 | 112.6 | 41.0 | -41.8 |
| TR5 | D9241A | -240 | 90 | CH5 | 224.4 | 47.0 | -29.5 | 109.2 | 41.0 | -42.7 |
| TR6 | D9241A | -168 | 90 | CH6 | 209.5 | 46.5 | -29.0 | 117.6 | 41.4 | -39.4 |
| TR7 | WDI | -350 | 90 | CH7 | 76.0 | 37.6 | -38.7 | 41.4 | 32.3 | -58.5 |
| | | | | | | | | | | |
| for set TR0-TR6 | | | | average | 214.2 | 46.7 | -26.5 | 114.4 | 41.2 | -39.9 |
| | | | | st. dev. | 12.6 | 0.4 | 2.5 | 3.5 | 0.1 | 1.9 |

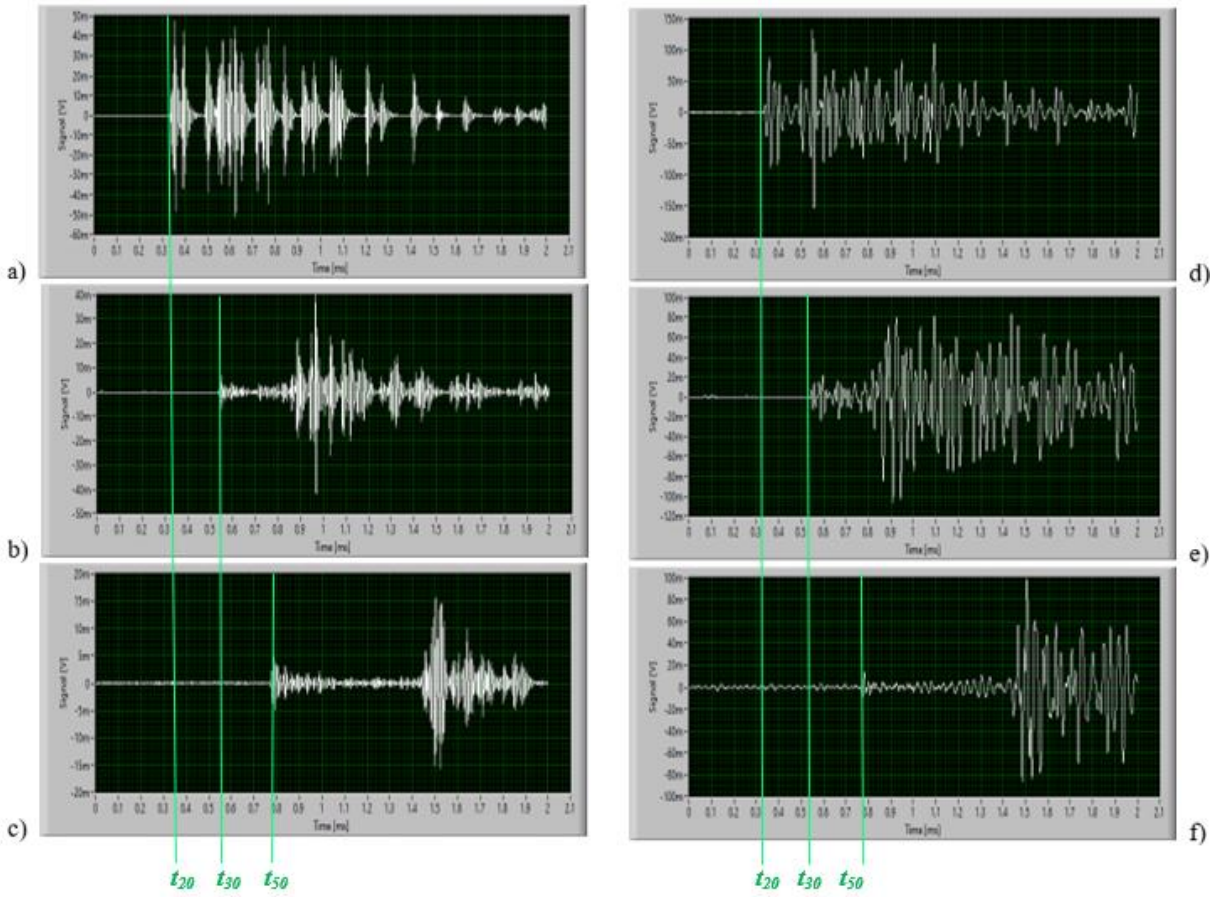


Fig. 3. Signals recorded in different measurement channels during the Hsu-Nielsen test performed next to the TR2 sensor and after filtering of the signals in the selected frequency bands: 100-200 kHz - a) CH2, b) CH3, c) CH5; 20-100 kHz - d) CH2; e) CH3; f) CH5

Rys. 3. Sygnały zarejestrowane w różnych kanałach pomiarowych podczas testu Hsu-Nielsena wykonywanego przy czujniku TR2 i następnie poddane filtracji w wybranych pasmach częstotliwości: 100-200 kHz - a) CH2, b) CH3, c) CH5; 20-100 kHz - d) CH2; e) CH3; f) CH5

Table 2

Peak-to-peak amplitudes $U_{pp}$ and ADC descriptor values for the AE signals recorded with sensors TR3 in CH3 during operation of Hsu-Nielsen sources located next to the different AE sensors

| Name of H-Nn | H-Nn location | | Results of measuring with TR3 sensor within CH3 for different H-Nn tests | | | |
|---|---|---|---|---|---|---|
| | *X* | *Y* | 20 - 100 kHz | | 100-200 kHz | |
| | | | *Upp* | ADC | *Upp* | ADC |
| | cm | cm | mV | a.u. | mV | a.u. |
| H-N1 | -545 | 95 | 189.2 | -30.6 | 67.2 | -78.2 |
| H-N2 | -481 | 95 | 205.4 | -27.9 | 84.3 | -67.2 |
| H-N3 | -350 | 95 | 228.0 | -21.0 | 121.4 | -37.4 |
| H-N4 | -290 | 95 | 220.6 | -23.5 | 81.6 | -54.5 |
| H-N5 | -240 | 95 | 201.2 | -24.9 | 72.4 | -63.2 |
| H-N6 | -168 | 95 | 184.2 | -29.0 | 65.8 | -71.7 |

### 21.4.2. Maps of the ADC descriptors on the side walls of the transformer tank along with the location of areas with increased AE activity in selected frequency bands

The first stage of analyzing the recorded data was the analysis in the domain of the threshold of discrimination. Each signal was filtered in a selected frequency band and then for each signal author's original AE descriptor with the acronym ADC [9, 16] was calculated. The mean value and mean standard deviation were calculated for all signals recorded at one measuring point. The *X*, *Y* coordinates of the measurement points and the calculated mean values of the ADC descriptor at a given measurement point are input data for the construction of ADC descriptor maps on the side walls of the transformer tank. These maps are built by the kriging method because kriging is considered to be the best method of estimating the values of spatial variables in geostatistics.

In accordance with the developed methodology of conducting the analysis of measurement data, maps of the ADC descriptor have been prepared in the frequency bands 100-200 kHz and 20-100 kHz. The calculated maps of the ADC descriptors on the side walls of the transformer tank are presented in Fig. 4. As can be seen in Fig. 4, the grids developed for the maps are the side walls of the tested transformer tank, where each point has coordinates (*X*, *Y*) given in centimeters:

*X* − position running along the transformer tank, (0 - the point opposite the centre of the tap changer (TC), positive *X* values for the part of the tank from the low voltage bushing side (LVbs), negative *X* values for the part of the tank from the high voltage bushing side (HVbs),

*Y* − height running up the tank (0 - bottom of the tank).

The map drawn after filtering of the signal in the 100-200 kHz band (Fig. 4a) shows one area L1 where AE signals with increased activity were recorded. On the map drawn after filtering of the signal in the 100-200 kHz band (Fig. 4b) three such areas can be seen (L2, L3 and L4).

The analysis of the properties of the signals recorded at the measurement points located in the L1 area visible in Fig. 4a were used to identify PD signals and locate PD sources (analysis of the recorded signals in the 100-200 kHz band).

The analysis of the properties of the signals recorded at the measurement points located in the L2-L4 areas visible in Fig. 4b were used to identify signals from the magnetization processes taking place in the magnetic circuit of the transformer and locate their sources (analysis of the recorded signals in the 20-100 kHz band).

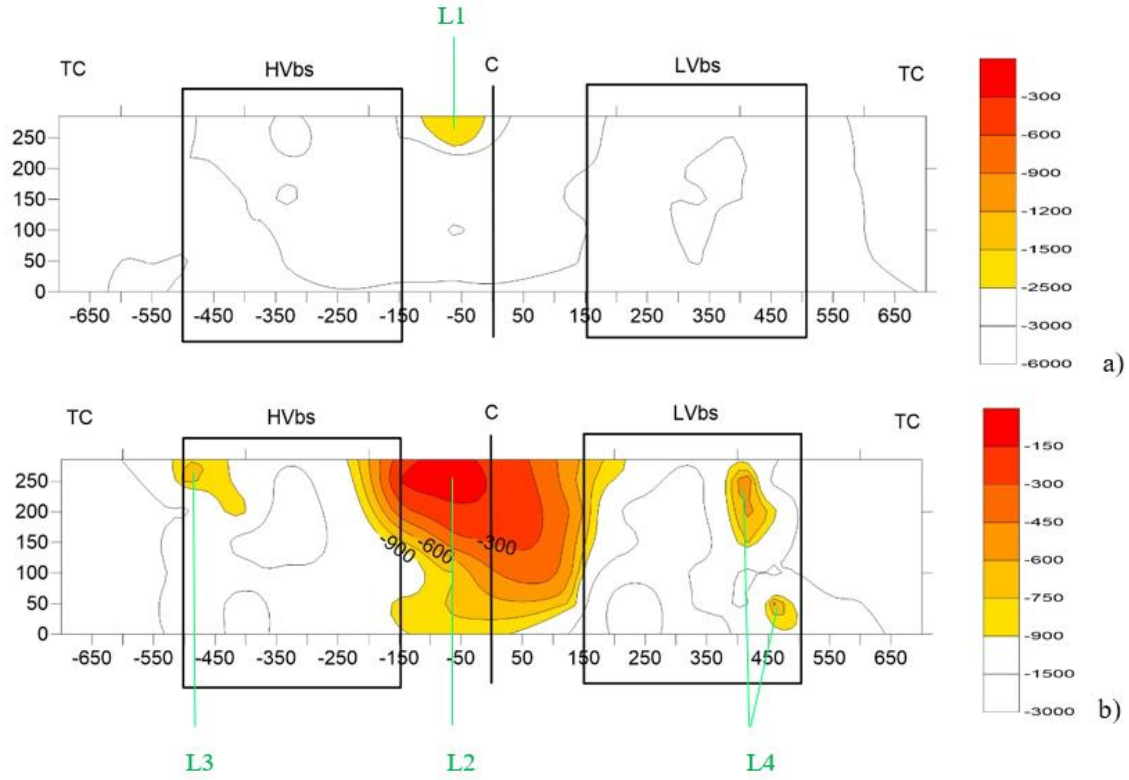


Fig. 4. Maps of the ADC descriptor values on the lateral walls of the tank of the tested transformer within the chosen frequency bands: a) 100-200 kHz; b) 20-100 kHz, with the localized areas L1, L2, L3 and L4. Description of the points within the maps: (*X*; *Y*) in centimeters - coordinates of the points at the side walls of the tested transformer tank : *X* - horizontal coordinate along the transformer tank, (0 - the point opposite to the center of the tap changer (TC), positive *X* values for part of the tank from the low voltage bushing side (LVbs), negative *X* values for part of the tank from the high voltage side (HVbs), *Y* - vertical coordinate up the tank (0 - bottom of the tank)

Rys. 4. Mapy wartości deskryptora ADC na ścianach bocznych kadzi badanego transformatora w wybranych pasmach częstotliwości: a) 100-200 kHz; b) 20-100 kHz, ze zlokalizowanymi obszarami L1, L2, L3 i L4. Opis punktów na mapach: (*X; Y*) w centymetrach - współrzędne punktów na ścianach bocznych badanego kadzi transformatora: *X* - współrzędna pozioma wzdłuż kadzi transformatora, (0 - punkt przeciwległy do środka przełącznik zaczepów (TC), dodatnie wartości X dla części zbiornika od strony tulei niskiego napięcia (LVbs), ujemne wartości X dla części zbiornika od strony wysokiego napięcia (HVbs), *Y* - współrzędna pionowa w górę zbiornika (0 - dno zbiornika)

### 21.4.3. Properties of AE signals from localized area with increased AE activity on ADC descriptor map in the 100-200 kHz band

In the area indicated by L1 in Fig. 4, the measurement point closest to the maximum of AE activity was located and ADC descriptors were calculated for the signals recorded at this measurement point. The mean value of the ADC descriptor is -1169 and the mean standard deviation of this value is 748, which means that the recorded processes are unstable. The vast majority of the recorded signals have the properties defined by the characteristics shown in Fig. 5. Within Fig. 5 , there are the following characteristics: phase-amplitude characteristics of the signal module and the Short-Time Fourier Transform (STFT) spectrogram. The phase-

time characteristic is obtained in the following way: the transient signal's absolute value is calculated, the modified signal is divided into fragments with a length of one supply voltage period and ultimately these fragments are folded one after the other and stitched as the phase-time characteristic. The "tunnel" in such a characteristic confirms the periodic character of the analyzed signal. The STFT spectrogram of the signal is calculated as the average spectrogram of all the spectrograms that are calculated for the signal in successive periods of the supply voltage.

Fig. 5 shows the characteristics for the vast majority of recorded signals. Within the signal there are numerous time structures that occur four times during the supply voltage's period (they occur at the times when the supply voltage's phases are close to the values of 50° and 230° as well as 130° and 310°). These time structures do not come from partial discharges and they are magnetoacoustic emission signals with harmonic components that are higher than 100 kHz [16]. These structures produce four "tunnels" in the amplitude-phase characteristics of the signal module and four areas on the STFT spectrograms.

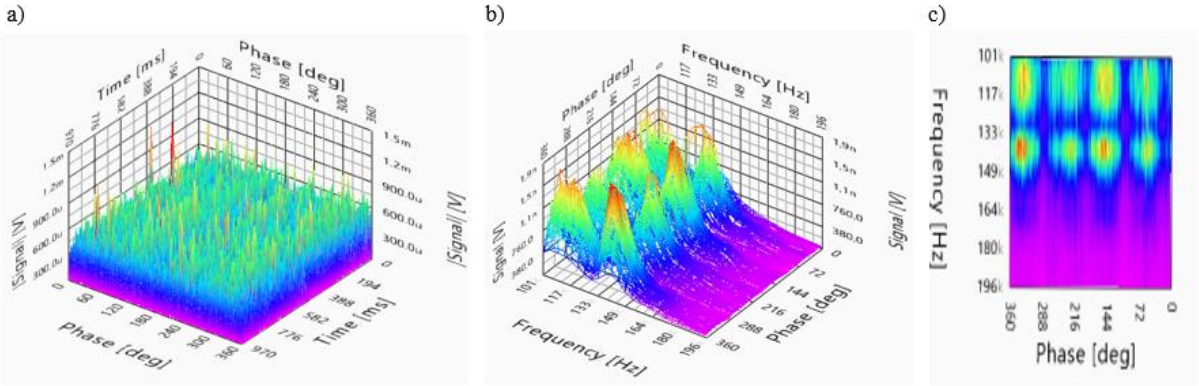


Fig. 5. Acoustic image of a selected AE signal (representing most of recorded signals) from L1 area within the map from Fig. 4a: a) phase-time characteristic, b) averaged 3D STFT spectrogram, c) averaged 2D STFT spectrogram. AE signal parameters: ADC = -3020, $U_{pp}$ = 3.68 mV, $U_{rms}$ = 0.15 mV

Rys. 5. Obraz akustyczny wybranego sygnału EA (reprezentującego większość zarejestrowanych sygnałów) z obszaru L1 w obrębie mapy z rys. 4a: a) charakterystyka fazowo-czasowa, b) uśredniony spektrogram 3D STFT, c) uśredniony spektrogram 2D STFT. Parametry sygnału EA: ADC = -3020, $U_{pp}$ = 3,68 mV, $U_{rms}$ = 0,15 mV

In the registered signals there are only individual signals having the characteristics of the type shown in Fig. 6 in which single time structures with large amplitude occur. For these few large signals, the following details are important:

- the signals only occur at certain phase intervals of the supply voltage,
- the signals have high ADC descriptor values,
- these are not signals that occur periodically as the supply voltage changes.

In addition to these facts, from the location of L1 area, it can be concluded that these signals originate from PDs generated in bubbles that are generated in the circulating cooling medium. As they are not in insulation, they are not significant in the further operation of the tested transformer. The transient signal of such a signal fragment that is registered with a wideband AE sensor is shown in Fig. 7. The estimated duration of AE burst structure is about 30 μs and it is not a signal coming directly from a PD but coming from a PD and then subjected to transformation at the input of the transformer tank material.

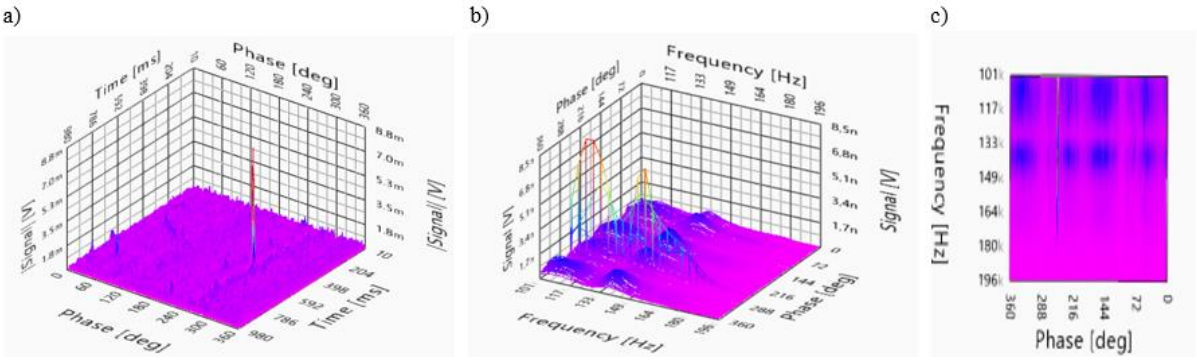


Fig. 6. Acoustic image of a selected AE signal (representing a few of recorded signals) from L1 area within the map from Fig. 4a: a) phase-time characteristic, b) averaged 3D STFT spectrogram, c) averaged 2D STFT spectrogram. AE signal parameters: ADC = -300, $U_{pp}$ = 18.28 mV, $U_{rms}$ = 0.14 mV

Rys. 6. Obraz akustyczny wybranego sygnału AE (reprezentującego kilka zarejestrowanych sygnałów) z obszaru L1 w obrębie mapy z rys. 4a: a) charakterystyka fazowo-czasowa, b) uśredniony spektrogram 3D STFT, c) uśredniony spektrogram 2D STFT. Parametry sygnału AE: ADC = -300, $U_{pp}$ = 18,28 mV, $U_{rms}$ = 0,14 mV

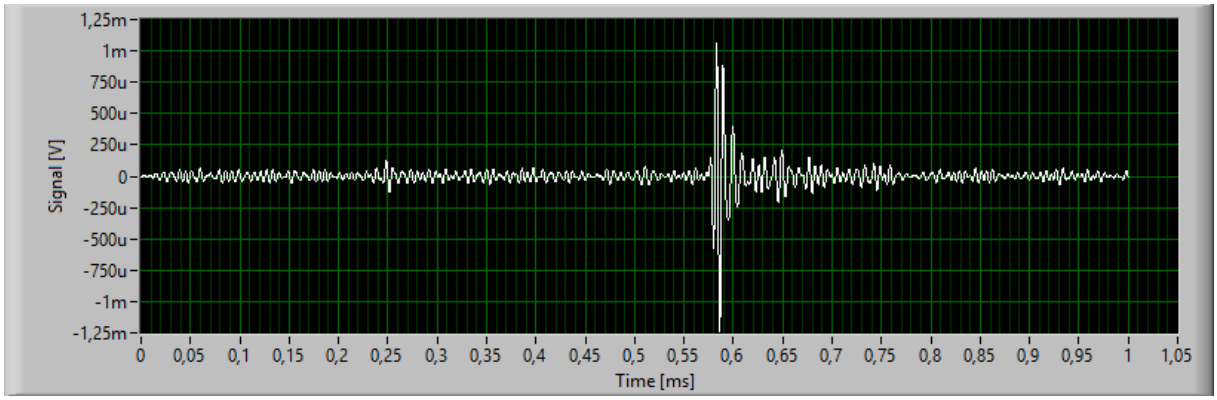


Fig. 7. The transient signal of a fragment of the AE signal (from Fig. 6) registered with a WDI type wideband sensor, the estimated duration of AE burst structure within signal: $\Delta t$ = 30μs

Rys. 7. Fragment sygnału EA (z rys. 6) zarejestrowanego za pomocą czujnika szerokopasmowego typu WDI, szacowany czas trwania fragmentu typu impulsowego sygnału EA: $\Delta t$ = 30μs

### 21.4.4. Properties of AE signals from localized area with increased AE activity on ADC descriptor map in the 20-100 kHz band

In the area indicated by L2 in Fig. 4b, the measurement point closest to the maximum of AE activity was located and ADC descriptors were calculated for the signals recorded at this measurement point. The mean value of the ADC descriptor is -394 and the mean standard deviation of this value is 54, which means that the recorded processes are stable. The processes are also stable in the L3 and L4 areas. An acoustic image of an exemplary representative AE signal from area L2 is shown in Fig. 8.

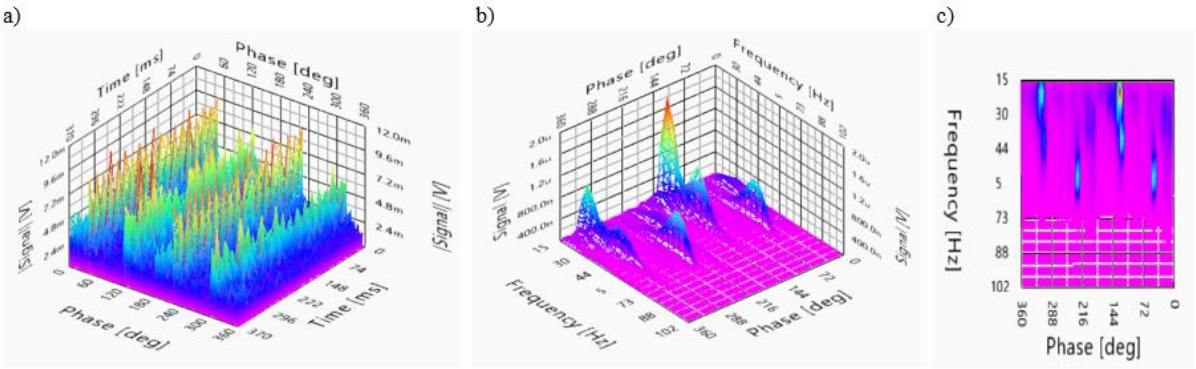


Fig. 8. Acoustic image of a selected AE signal from L2 area within the map from Fig. 4b (after filtration of AE signal within the 20-100 kHz band: a) phase-time characteristic, b) averaged 3D STFT spectrogram, c) averaged 2D STFT spectrogram.
AE signal parameters: ADC = -351, $U_{pp}$ = 22.64 mV, $U_{rms}$ = 1.19 mV

Rys. 8. Obraz akustyczny wybranego sygnału AE z obszaru L2 w obrębie mapy z rys. 4b (po przefiltrowaniu sygnału EA w paśmie 20-100 kHz: a) charakterystyka fazowo-czasowa, b) uśredniony spektrogram 3D STFT, c) uśredniony spektrogram 2D STFT.
Parametry sygnału EA: ADC = -351, $U_{pp}$ = 22,64 mV, $U_{rms}$ = 1,19 mV

A detailed analysis of the characteristics presented in Fig. 8 indicated the presence of the following signal properties:

- four "tunnels" on the phase-time characteristic – the signal has periodic properties, within four bands of the supply voltage's phases,
- there are four structures on the STFT spectrogram that describe the frequency properties of the periodic signals.

These four structures can be divided into two groups of two signals each:

- in one group there are signals where the main band of the signal is 45-65 kHz, the estimated duration of such a structure is 100 μs; these signals occur when the supply voltage phase is around 50° or 230° (Fig. 9);
- in the second group there are signals for which the main band of the signal is 35-45 kHz, the estimated duration of AE burst structure is about 200 μs; these signals occur when the supply voltage phase is around 130° or 310° (Fig. 10).

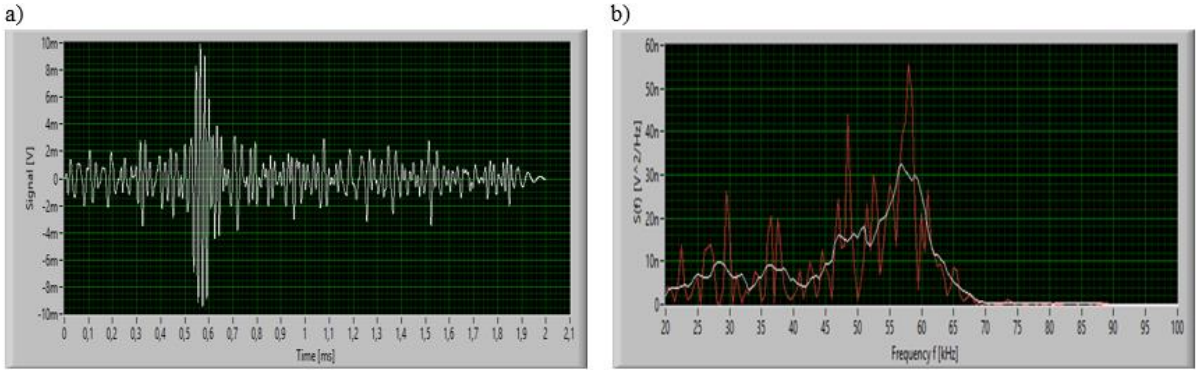


Fig. 9. Transient signal for the fragment of signal recorded within L2 area when the supply voltage phase is around 50° (a) together with its Fourier transform (b); the estimated duration of AE burst structure within signal: $\Delta t$ = 130 μs

Rys. 9. Fragment sygnału EA zarejestrowanego w obszarze L2, gdy faza napięcia zasilania wynosi około 50° (a) wraz z jego transformatą Fouriera (b); szacowany czas trwania fragmentu typu impulsowego sygnału EA: $\Delta t$ = 130 μs

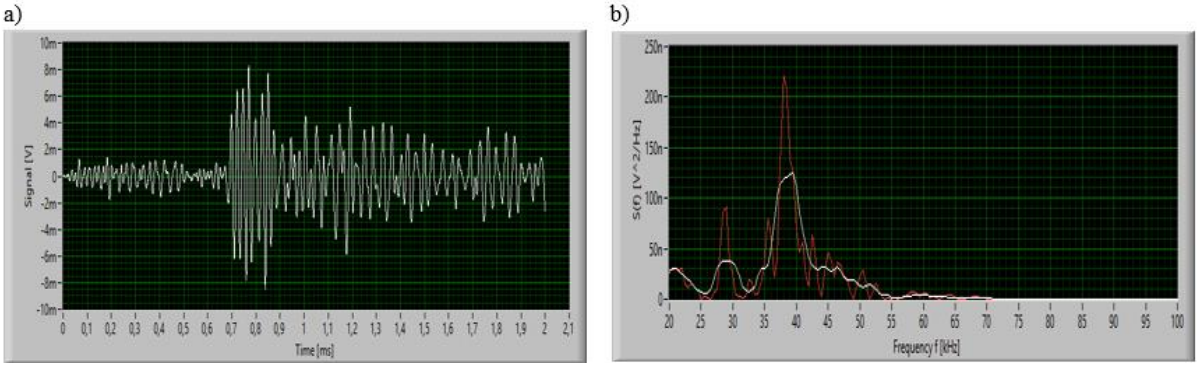


Fig. 10. Transient signal for the fragment of signal recorded within L2 area when the supply voltage phase is around 130° (a) together with its Fourier transform (b); the estimated duration of AE burst structure within signal: $\Delta t$ = 200 μs

Rys. 10. Fragment sygnału EA zarejestrowanego w obszarze L2, gdy faza napięcia zasilania wynosi około 130° (a) wraz z jego transformatą Fouriera (b); szacowany czas trwania fragmentu typu impulsowego sygnału EA: $\Delta t$ = 200 μs

The results of a detailed signal analysis presented above indicate that the recorded signals are magnetoacoustic emission signals [14-16]. The processes of magnetization of materials take place in the entire magnetic circuit of the transformer, therefore the areas located in Fig. 4b should be identified as areas where MAE has high activity. Since MAE is closely related to the hysteresis loop for magnetic materials, and the area of the hysteresis curve is associated with energy losses, among others, causing a local increase in the temperature of the material, the results of these tests should be treated as additional information indicating which areas of the transformer should be tested for the purpose of determining the temperature

distribution in the tested transformer [23] and further research aimed at examining the quality of the magnetic material in the localized areas marked as L2-L4.

## 21.5. Conclusions

The study presents the research methodology for oil power transformers including identification of signals from partial discharges and magnetization processes taking place in the magnetic circuit of the transformer and the location of their sources.

The methodology covers the creation of a network of measuring points on the side walls of the transformer tank, the installation of a set of eight sensors (operating in eight measuring lines of the 8AE-PD system) at subsequent measuring points (with each time checking the quality of the installation using Hsu-Nielsen tests), carrying out measurements after confirming that installation quality that meets the requirements of the PN-EN 14584: 2013-07 Standard and analysis of recorded signals.

The paper presents an analysis of the results of tests carried out on a selected transformer, in which partial discharges were found in the area defined as L1 area and magnetoacoustic emission in areas defined as L2-L4 areas. The results of localization of sources of partial discharges and magnetoacoustic emission with high activity are also shown.

The registered AE signals derived from PDs were single signals that did not occur periodically as the supply voltage changed. The signals were not located in the transformer insulation system but were generated in bubbles appearing in the circulating cooling medium. Thus, the PD sources present in the transformer during the test were not significant in the further operation of the tested transformer.

Areas marked as L2-L4 are areas where MAE has high activity and should be tested for the purpose of determining the temperature distribution in the tested transformer and further research aimed at examining the quality of the magnetic material in these localized areas.

The results of a detailed signal analysis presented above indicate that the recorded signals are magnetoacoustic emission signals [14-16]. The processes of magnetization of materials take place in the entire magnetic circuit of the transformer, so the areas located in Fig. 4b should be identified as areas where MAE has high activity. Since MAE is closely related to the hysteresis loop for magnetic materials, and the area of the hysteresis curve is associated with energy losses, among others, causing a local increase in the temperature of the material, the results of these tests should be treated as additional information indicating which areas of the transformer should be tested for the purpose of determining the temperature distribution in the tested transformer [23] and further research aimed at examining the quality of the magnetic material in the localized areas marked as L2-L4.

## Bibliography

1. The Framework Instruction for Operation of Transformers (in Polish). Energopomiar-Elektryka, Gliwice 2001, ISBN 83-916040-0-4.
2. Kapinos J., Glinka T., Drak B.: Typical causes of operational failures of power transformers (in Polish). Przegląd Elektrotechniczny 90(1), 2014, 186-189.
3. Wu M., Cao H., Cao J., Nguyen H., Gomes J.B., Krishnaswamy S.P.: An overview of state-of-the-art partial discharge analysis techniques for condition monitoring. IEEE Electrical Insulation Magazine 31(6), 2015, 22-35.
4. Markalous S., Tenbohlen S., Feser K.: Detection and Location of Partial Discharges in Power Transformers using Acoustic and Electromagnetic Signals. IEEE Trans. Dielectr. Electr. Insul. 15, 2008, 1576-1583.
5. Witos F., Olszewska A., Szerszeń G.: Analysis of properties characteristic for acoustic emission signals recorded on-line in power oil transformers. Acta Phys. Pol. A 120(4), 2011, 759-762.
6. Olszewska A., Witos F.: Location of partial discharge sources and analysis of signals in chosen power oil transformers by means of acoustic emission method. Acta Phys. Pol. A 122, 2012, 921-926.
7. Búa-Núñez I., Posada-Román J.E., Rubio-Serrano J., Garcia-Souto J.A.: Instrumentation System for Location of Partial Discharges Using Acoustic Detection With Piezoelectric Transducers and Optical Fiber Sensors. IEEE Trans. Instrum. Meas. 63, 2014, 1002-1013.
8. Sikorski W., Walczak K., Gil W., Szymczak C.: On-Line Partial Discharge Monitoring System for Power Transformers Based on the Simultaneous Detection of High Frequency, Ultra-High Frequency, and Acoustic Emission Signals. Energies 13, 2020, 3271-3307.
9. Witos F., Opilski Z., Szerszeń G., Setkiewicz M.: The 8AE-PD computer measurement system for registration and analysis of acoustic emission signals generated by partial discharges in oil power transformer. Metrol. Meas. Syst. 26, 2019, 404-418.
10. Witos F., Opilski Z., Szerszeń G., Setkiewicz M., Olszewska A., Duda D., Maźniewski K., Szadkowski M.: Calibration and laboratory testing of computer measuring system 8AE-PD dedicated for analysis of acoustic emission signals generated by partial discharges within oil power transformers. Arch. Acoust. 42, 2017, 297-311.
11. Bartnikas R.: Partial Discharges - Their Mechanism, Detection and Measurement. IEEE Trans. Dielectr. Electr. Insul. 9, 2002, 763–808.
12. Boczar T.: Identification of a Specific Type of Partial Discharges form Acoustic Emission Frequency Spectra. IEEE Trans. Dielectr. Electr. Insul. 8, 2001, 598-606.

13. Harbaji M., Shaban K., El-Hag A.: Classification of Common Partial Discharge Types in Oil-paper Insulation System using Acoustic Signals. IEEE Trans. Dielectr. Electr. Insul. 22, 2015, 1674-1683.
14. Augustyniak B., Piotrowski L., Chmielewski M., Sablik M.J.: Nondestructive characterization of 2Cr-1Mo steel quality using magnetoacoustic emission. IEEE Trans. Magn. 38(5), 2002, 3207-3209.
15. Wilson J., Tian. G.Y., Moorthy V., Shaw B.A.: Magneto-Acoustic Emission and Magnetic Barkhausen Emission for Case Depth Measurement in En36 Gear Steel. IEEE Trans. Magn. 45(1), 2009, 177-183.
16. Olszewska A., Witos F.: Identification of acoustic emission signals originating from the core magnetization of power oil transformer. Arch. Acoust. 41(4), 2016, 798-812.
17. Witos F.: Properties of amplitude distributions of acoustic emission signals generated in pressure vessel during testing. Arch. Acoust. 44(3), 2019, 493-503.
18. Gacek Z., Szadkowski M., Malitowski G., Witos F., Olszewska A.: Unusual application of partial discharges to diagnose of high voltage power transformers. Acta Phys. Pol. A 120(4), 2011, 609-615.
19. Olszewska A., Witos F.: Location and identification of acoustic signals recorded in power oil transformers within the band of 20-180 kHz. Acta Phys. Pol. A 120(4), 2011, 709-712.
20. Witos F., Gacek Z.: Application of the joint electro-acoustic method for partial discharge investigations within a power transformer. Eur. Phys. J. Spec. Top. 154(1), 2008, 239-247.
21. Boczar T., Lorenc M.: The repeatability and reproducibility of calibrating signals generated by Hsu-Nielsen method. J. Phys. IV France 129, 2005, 97-103.
22. Markus G., Sause R.: Investigation of pencil-lead break as acoustic emission sources. J. Acoustic Emission 29, 2011, 184-196.
23. Lisowska-Lis A., Witos F., Szerszeń G.: Thermographic analysis of power oil transformer surface hot spot areas combined with analysis of acoustic signals recorded on line. Proc. of SPIE 11204, 2018, 112040B-4.